# Supporting Information

# Formation of Anisotropic Liquid Crystalline Nanoparticles via Polymerization Induced Hierarchical Self-Assembly

Song Guan,[†, §] Chen Zhang,[†] Wei Wen,[†] Ting Qu,[†] Xiaoxiong Zheng,[†] Yongbin Zhao,[‡] and Aihua Chen*[,†,§]

[†]School of Materials Science and Engineering, Beihang University, Beijing 100191, P. R. China
[‡]Shandong Oubo New Material Co Ltd, Shandong 257088, P. R. China
[§]Beijing Advanced Innovation Centre for Biomedical Engineering, Beihang University, Beijing 100191, P. R. China

## Table of Contents

# 1. Materials and methods

## 1.1 Materials

4-cyanopentanoic acid dithiobenzoate (CPADB, 97%, Aladdin), 4,4'-azobis(4-cyanovaleric acid) (ACVA, 98%, J&K Chemical), 1,1,3,3-tetramethylguanidine (TMG, 99%, Macklin), benzyl chloride (99%, Macklin), ethanol (99.8%, Aladdin), dimethyl sulfoxide (DMSO, 99.8%, Macklin), chlorobenzene (99%, Aladdin) were used as received. Methylacrylic acid (MAA, 99%, Aladdin) was purified by passing through a basic alumina oxide column prior to storage at -10 $^{o}$C. The 11-[4-(4-butylphenylazo)phenoxy]undecyl methacrylate (MAAz) monomer was synthesized following the previously reported method.[1]

## 1.2 Synthesis of PMAA macro-CTA via RAFT solution polymerization

In a typical RAFT solution polymerization for synthesis of PMAA$_{112}$ macro-CTA, MAA (10.32 g, 120 mmol), CPADB (0.28 g, 1.00 mmol), ACVA (56.1 mg, 0.20 mmol), and ethanol (10.32 g) were added to a reaction tube. The mixture was degassed by three freeze-pump-thaw cycles, and sealed under vacuum. The reaction tube was placed in an oil bath at 70 °C. After 5 h, the reaction was quenched by dipping the tube in ice/water and the tube was broken. The mixture was diluted with ethanol, precipitated in n-hexane 3 times. PMAA macro-CTA was purified via dialysis (MWCO 3 kg/mol) in ethanol for 3 days. Then dry under vacuum. The product was a pink solid (9.2 g, monomer conversion 89%). The DP was measured by $^{1}$H NMR in DMSO-$d6$ (DP=112).The $M_{n}$ and $M_{w}/M_{n}$ were measured by GPC ($M_{n}$=11.7 k, $M_{w}/M_{n}$=1.07).

## 1.3 Synthesis of PMAA-$b$-PMAAz block copolymer nanoparticles via RAFT dispersion polymerization

In a typical dispersion polymerization formulation targeting PMAA$_{112}$-$b$-PMAAz$_{150}$ at 20% w/w solids, PMAA$_{112}$ macro-CTA (0.1 g, 0.010 mmol), ACVA (0.58 mg, 0.002 mmol), MAAz (0.77 g, 1.56 mmol) and ethanol (3.48

g) were added to a reaction tube. The mixture was degassed by three freeze-pump-thaw cycles, and sealed under vacuum. The reaction tube was placed in an oil bath at 70 °C. After 12 h, the reaction was quenched by dipping the tube in ice/water and the tube was broken. The resulting block copolymer was characterized by using $^1$H NMR, DLS, AFM, SEM and TEM.

## 1.4 Chemical Modification of PMAA macro-CTA and PMAA-*b*-PMAAz block copolymer

For GPC studies, the carboxylic acid groups on the PMAA macro-CTA and PMAA-*b*-PMAAz block copolymer were fully esterified using benzyl chloride with TMG as a promoter, as reported by Bai and coworkers.[2] In a typical chemical modification of PMAA macro-CTA, PMAA (43 mg, 0.5 unit mmol) was dissolved in DMSO (1 mL). Then TMG (115 mg, 1 mmol) and benzyl chloride (95 mg, 0.75 mmol) were added. Then the mixture was stirred over night at room temperature. The resulting polymer was precipitated into a large amount of methanol, and collected by filtration and then drying under vacuum at 40 $^o$C. The chemical modification of PMAA-*b*-PMAAz block copolymer is similar with PMAA macro-CTA except the 75/25% w/w CHCl$_3$/DMSO mixtures as the solvent.

## 1.5 Photo-responsive of the PMAA-*b*-PMAAz nanoparticles prepared by PISA

A small aliquot mixture after PISA was diluted 10 times using ethanol. The mixture was irradiated by 360 nm UV light (OMRON, ZUV-H20MC) 1 hour with stirring. Then, the mixture was stored in a dark bottle. The morphologies and sizes were characterized by using TEM and DLS.

## 2. Characterization

**2.1 NMR spectroscopy.** NMR spectra were measured on a Bruker DMX spectrometer, operating at 400 MHz for $^1$H. The CPADB was characterized using CDCl$_3$ as the solvent. The PMAA macro-CTA were characterized using DMSO-*d6* as the solvent. The PMAA-*b*-PMAAz block copolymers were characterized using 75/25% w/w CDCl$_3$/DMSO-*d6* mixtures as the solvent to make sure the complete dissolution of the two blocks.

**2.2 Gel permeation chromatography (GPC).** The $M_n$ and $M_w/M_n$ ratios of polymers (have been fully esterified using benzyl chloride with TMG as a promoter) were performed on a Waters 2410 gel permeation chromatography (GPC) equipped with two columns (Styragel Column, HR 4, 5 μm, 7.8 mm x 300 mm, 5-600 K and Styragel Column, HR 2, 5 μm, 7.8 mm x 300 mm, 500-20 K).THF (HPLC) was used as the eluent with the flow rate of 1mL/min. Molecular weight was calibrated by a series of monodisperse polystyrene standards.

**2.3 Transmission electron microscopy (TEM).** One drop of the dispersions with proper concentration in ethanol was deposited on a carbon-coated copper grid. The solvent was evaporated at room temperature for 1-2 d.The TEM samples obtained were stained by RuO$_4$. TEM images were obtained with a JEM-2100 microscope, operating at 200 kV.

**2.4 Scanning electron microscope (SEM).** One drop of the dispersions with proper concentration in ethanol was deposited on a copper grid. The solvent was evaporated at room temperature for 1-2 d. The SEM samples were gilded before the observation. The SEM images were acquired using Hitachi S4800 field emission scanning electron microscope at 5 kV.

**2.5 Atomic force microscopy (AFM).** One drop of the dispersions with proper concentration in ethanol was deposited on a cleansed silicon wafer. The solvent was

evaporated at room temperature for 1-2 d. AFM height images were collect by using a Bruker Resolve probe microscope under tapping mode.

**2.6 Dynamic light scattering (DLS).** DLS measurements were conducted using a Shandong Naikete NKT-N9 instrument equipped with a 532 nm He-Ne laser at 25 $^{\circ}$C. The hydrodynamic sizes of the nanoparticles in ethanol were characterized by analyzing the scattering light at 90°angle.

**2.7 Differential scanning calorimetry (DSC).** The mixture after PISA was volatilized 48 h in room temperature removing ethanol. Then, unreacted monomers and other impurities were removed by Soxhlet extraction 48 h in methanol. DSC analyses were measured using NETZSCH DSC214 instrument calibrated using indium standards. The DSC samples were scanned under air flow from 25 $^{\circ}$C to 200 $^{\circ}$C at a scanning rate 10 $^{\circ}$C /min. The data of first cooling processes and second heating processes were recorded.

**2.8 Small-angle x-ray scattering (SAXS).** A small aliquot mixture after PISA volatilized 48 h in room temperature removing ethanol. Then grinded before measured. SAXS was measured using a Anton-Paar SAXS mc2 diffractometer with Cu Kα radiation (λ=0.154 nm).

**2.9 Temperature-dependent polarized optical microscopic (POM).** A small aliquot mixture after PISA was dropped to the glass slide, volatilized 48 h in room temperature removing ethanol. POM experiments were done using Shang Guang 59XF microscope fitted with a Shang Guang XRD thermo-control system.

# 3. Supporting figures and table

## 3.1 Synthesis of PMAA$_m$-*b*-PMAAz$_n$ via RAFT dispersion polymerization
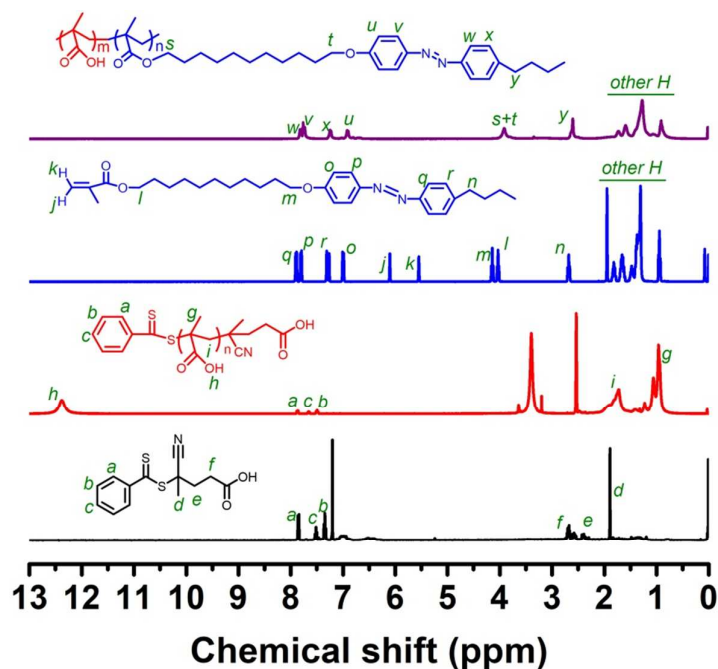


**Figure S1.** Chemical structures and typical $^1$H NMR spectra of CPADB, PMAA macro-CTA, MAAz monomer and the PMAA-*b*-PMAAz block copolymer synthesized via RAFT dispersion polymerization.
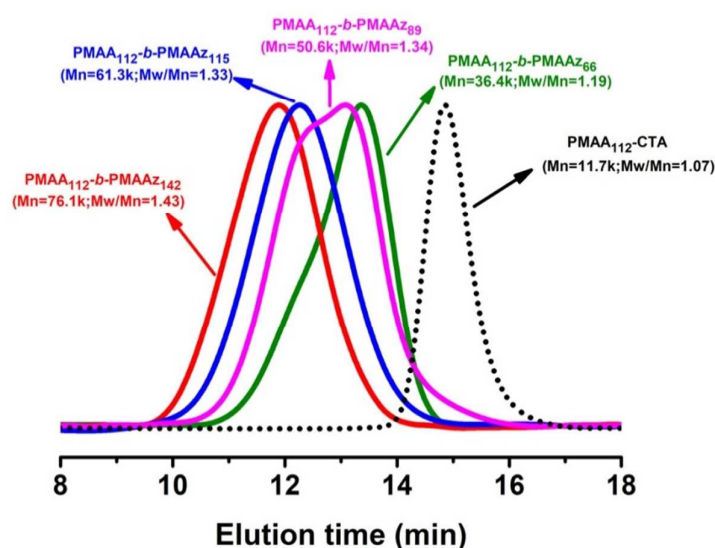


**Figure S2.** GPC traces of the PMAA$_{112}$ macro-CTA and a series of corresponding PMAA$_{112}$-*b*-PMAAz$_n$ block copolymers (THF, polystyrene standards) synthesized via

6

RAFT dispersion polymerization at 20% w/w in ethanol at 70 $^{\circ}$C. All of the polymers were fully esterified using benzyl chloride with TMG as a promoter.
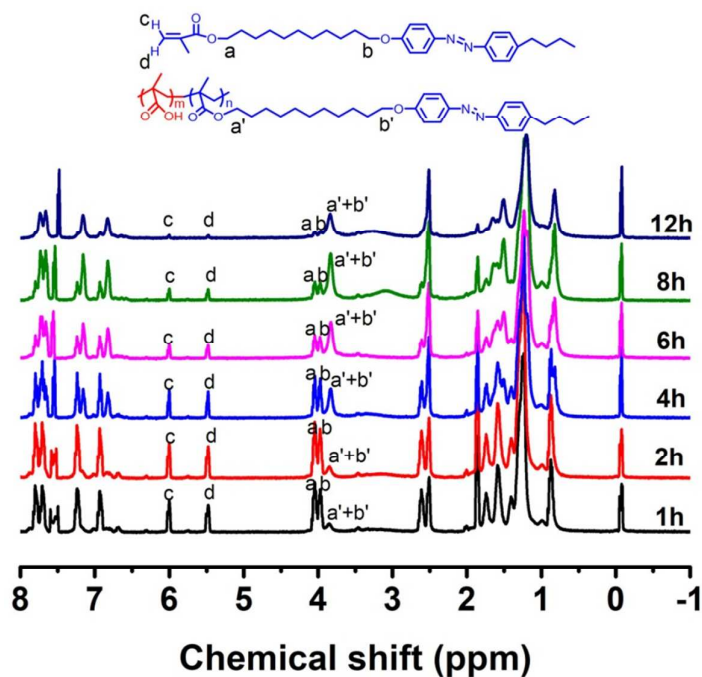


**Figure S3.** ^{1}H NMR spectra of the PMAA$_{75}$-b-PMAAz$_n$ block copolymers with different polymerization time. Target block copolymer composition was PMAA$_{75}$-b-PMAAz$_{150}$. Conditions: [macro-CTA]/[AIBN] molar ratio= 5.0; total solids concentration = 20% w/w.

The peaks a, b, c, d and a', b' are selected as representative peaks. The areas of a, b, c, d is getting smaller with increasing of the polymerization time. Reversely, the areas of a' + b' are getting larger with increasing of the polymerization time. It indicates that the MAAz monomers are polymerized effectively in this condition.

7
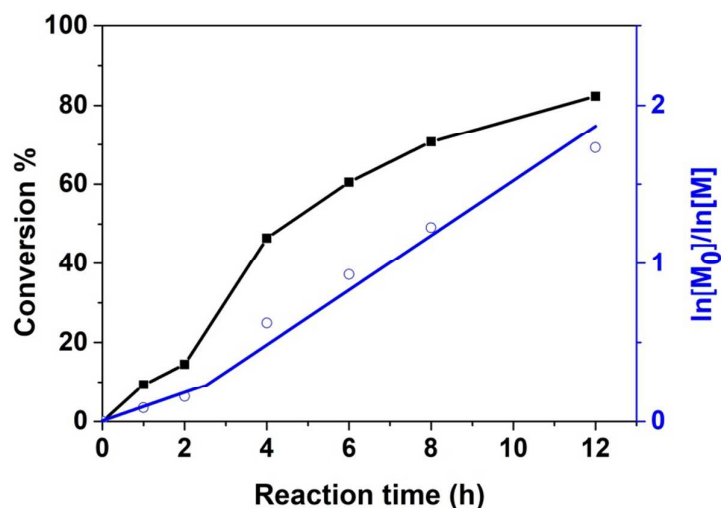
**Figure S4.** Monomer conversion-time plot and the corresponding semilogarithmic plot for the RAFT dispersion polymerization of MAAz. Target block copolymer composition is $PMAA_{75}$-$b$-$PMAAz_{150}$. Conditions: [macro-CTA]/[AIBN] molar ratio= 5.0; total solids concentration = 20% w/w; reaction temperature=70 $^{o}$C.
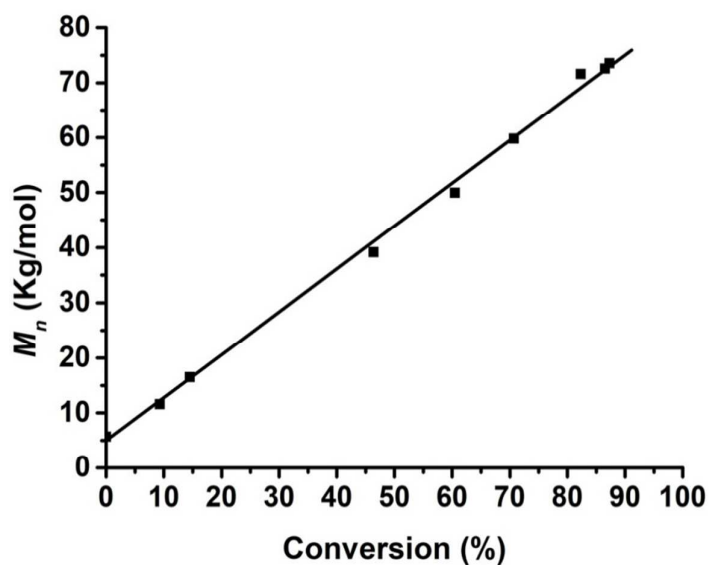


**Figure S5.** Number-average molecular weight-conversion plot for the RAFT dispersion polymerization of MAAz. Target block copolymer composition is $PMAA_{75}$-$b$-$PMAAz_{150}$. Conditions: [macro-CTA]/[AIBN] molar ratio= 5.0; total solids concentration = 20% w/w; Reaction temperature=70 $^{o}$C.

**Table S1.** Summary of DP, molecular weight, final morphology and particle size obtained from a series of PMAA-*b*-PMAAz block copolymers synthesized via RAFT dispersion polymerization at 70 °C in ethanol[a].

| Sample | DP of PMAA [b] | DP of PMAAz [c] | $M_n$ [c] (g/mol) | Mass fraction of PMAAz (%)[d] | GPC $M_n$ | GPC $M_w/M_n$ | Morphology[e] | DLS[f] Diam (nm) | DLS[f] PDI |
|---|---|---|---|---|---|---|---|---|---|
| 1 | 112 | 66 | 42100 | 77 | 36400 | 1.19 | cuboid | 108 | 0.188 |
| 2 | 112 | 89 | 53400 | 82 | 50600 | 1.34 | short belt | 186 | 0.217 |
| 3 | 112 | 115 | 66200 | 85 | 61300 | 1.33 | lamella | 297 | 0.366 |
| 4 | 112 | 142 | 79500 | 88 | 76100 | 1.43 | ellipsoidal vesicle | 335 | 0.130 |
| 5 | 75 | 48 | 30100 | 78 | 29300 | 1.21 | cuboid | 111 | 0.212 |
| 6 | 75 | 65 | 38400 | 83 | 34900 | 1.20 | short belt | 248 | 0.289 |
| 7 | 75 | 84 | 47800 | 86 | 43600 | 1.42 | lamella | 393 | 0.375 |
| 8 | 75 | 123 | 67000 | 90 | 54500 | 1.49 | vesicle | 876 | 0.685 |
| 9 | 38 | 15 | 10600 | 70 | 11300 | 1.16 | worm + lamella | 243 | 0.484 |
| 10 | 38 | 18 | 12100 | 73 | 13100 | 1.20 | worm + lamella | 254 | 0.571 |
| 11 | 38 | 32 | 19000 | 83 | 17800 | 1.35 | vesicle | 395 | 0.166 |
| 12 | 38 | 44 | 25000 | 87 | 23900 | 1.32 | vesicle | 411 | 0.231 |
| 13 | 176 | 75 | 52000 | 71 | 49500 | 1.21 | sphere + worm | 217 | 0.276 |
| 14 | 176 | 87 | 57900 | 74 | 58100 | 1.18 | worm | 231 | 0.192 |
| 15 | 176 | 134 | 81100 | 81 | 75800 | 1.28 | worm | 352 | 0.206 |
| 16 | 176 | 190 | 108600 | 86 | 109700 | 1.45 | worm + lamella | 408 | 0.420 |
| 17 | 176 | 265 | 145500 | 90 | 138600 | 1.48 | precipitate | -- | -- |

a) Conditions: [macro-CTA]/[ACVA] molar ratio = 5.0; total solids concentration = 20% w/w.

b) Determined by ^{1}H NMR spectroscopy in DMSO-*d6*.

c) Determined by $^1$H NMR spectroscopy in 75/25%w/w CDCl$_3$/DMSO-*d6* mixtures.

d) LC weight fraction determined by $^1$H NMR.

e) The copolymer particle morphology is determined by TEM observations.

f) Intensity-average diameters were calculated using a cumulants analysis software provided by the instrument manufacturer. PDI denotes the polydispersity.
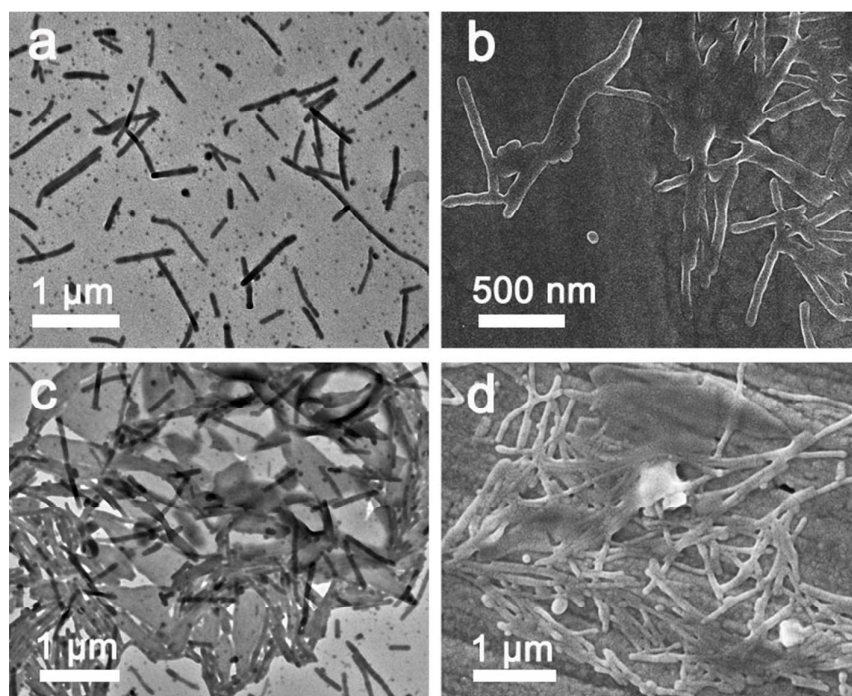
**3.2 Morphologies of different samples**
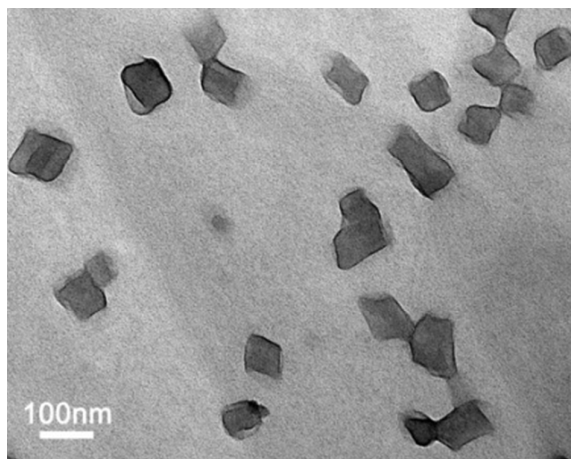


**Figure S6.** TEM enlarged image of the PMAA$_{75}$-*b*-PMAAz$_{48}$ nanoparticles.
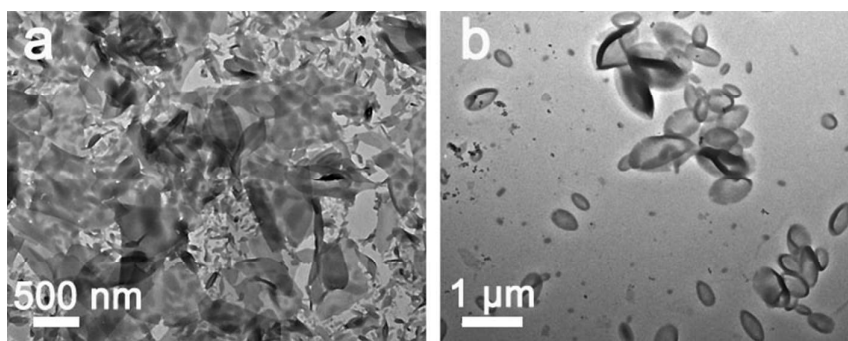


**Figure S7.** TEM images of the a) PMAA$_{38}$-*b*-PMAAz$_{18}$, and b) PMAA$_{38}$-*b*-PMAAz$_{32}$ nanoparticles, showing a hybrid morphology of lamellae and worms, and a vesicle morphology, respectively.

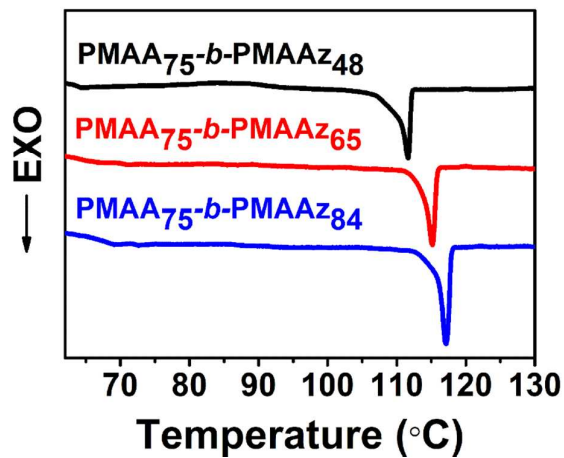**Figure S8.** TEM and the corresponding SEM images of the a-b) PMAA$_{176}$-$b$-PMAAz$_{134}$, and c-d) PMAA$_{176}$-$b$-PMAAz$_{190}$ nanoparticles, respectively.
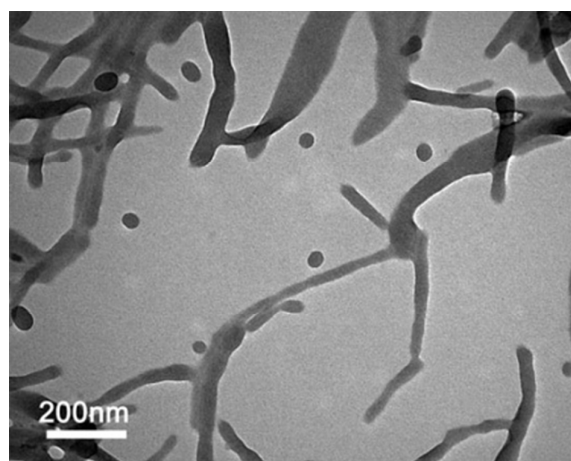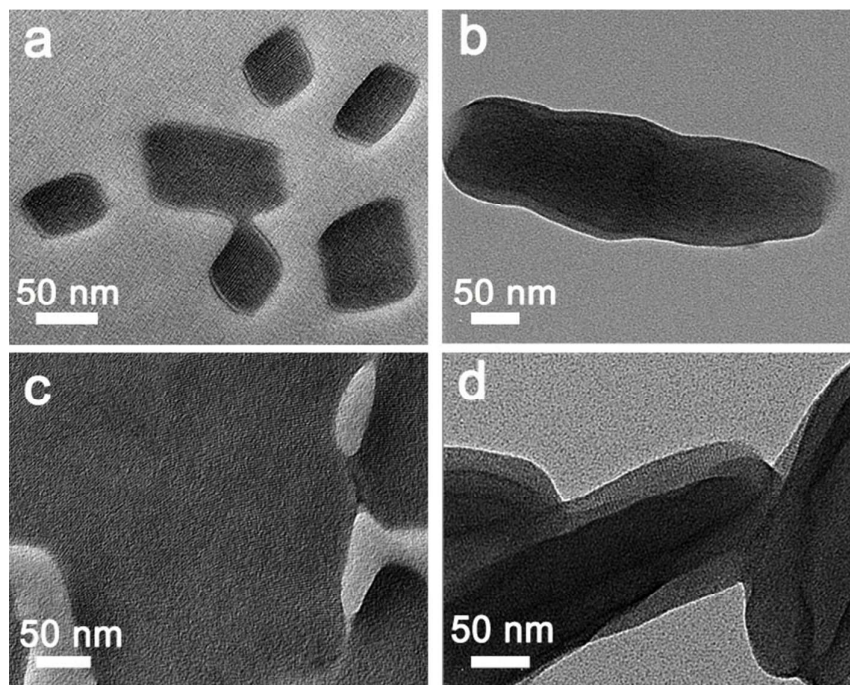


**Figure S9.** TEM image of the PMAA$_{176}$-$b$-PMAAz$_{75}$ nanoparticles.

**3.3 The mesomorphic properties of PMAA-*b*-PMAAz and nanoparticles**



**Figure S10.** DSC curves of the PMAA$_{75}$-*b*-PMAAz$_n$ block copolymers on the first cooling processes with a cooling rate of 10 $^{\circ}$C/min.



**Figure S11.** TEM magnified images of the PMAA$_{112}$-*b*-PMAAz$_n$ nanoparticles with various DP$_{PMAAz}$: a) PMAA$_{112}$-*b*-PMAAz$_{66}$, b) PMAA$_{112}$-*b*-PMAAz$_{89}$, c) PMAA$_{112}$-*b*-PMAAz$_{115}$, and d) PMAA$_{112}$-*b*-PMAAz$_{142}$. Smectic stripes can be observed in all images.

**3.4 The stabilization of PMAA-*b*-PMAAz nanoparticles via PISA**
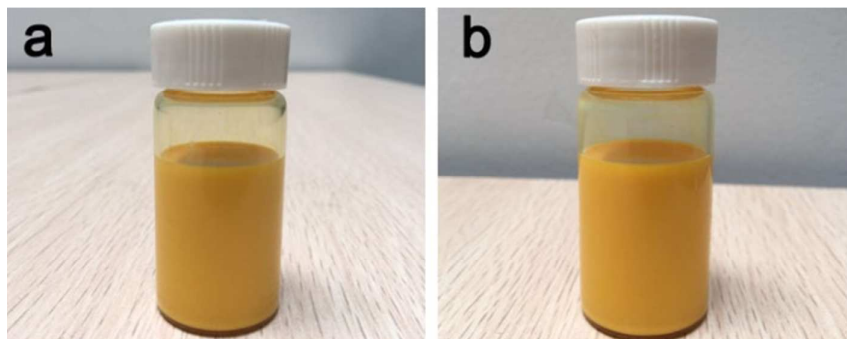


**Figure S12.** The photographs of the PMAA$_{112}$-*b*-PMAAz$_{142}$ nanoparticles: a) as-prepared b) after three months at room temperature.
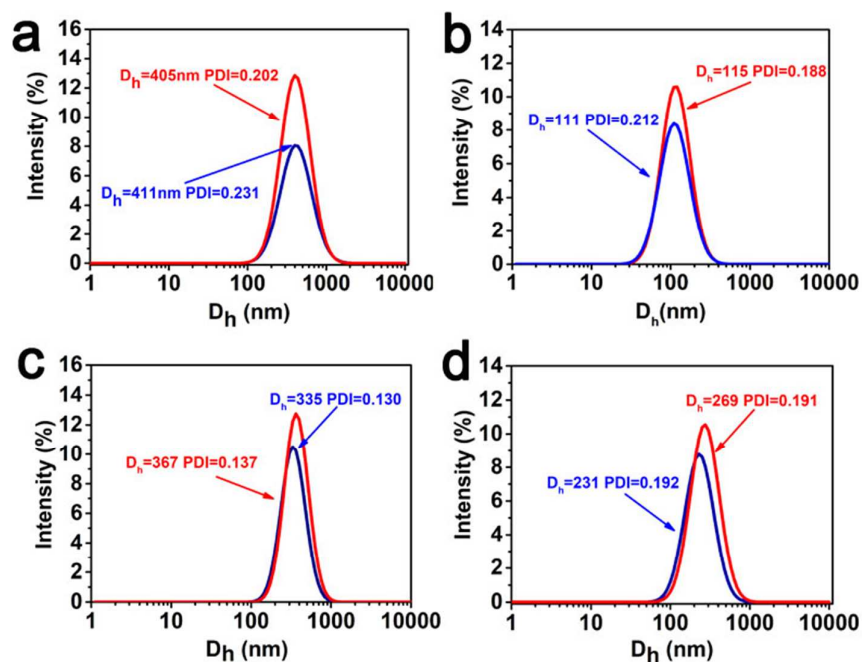


**Figure S13.** Typical Intensity-average size distributions (blue: as-prepared, red: after three months at room temperature) of the a) PMAA$_{38}$-PMAAz$_{44}$, b) PMAA$_{75}$-PMAAz$_{48}$, c) PMAA$_{112}$-PMAAz$_{142}$, and d) PMAA$_{176}$-PMAAz$_{87}$, respectively.

**3.5 Photo-responsive of the PMAA-*b*-PMAAz solution and the nanoparticles prepared by PISA**
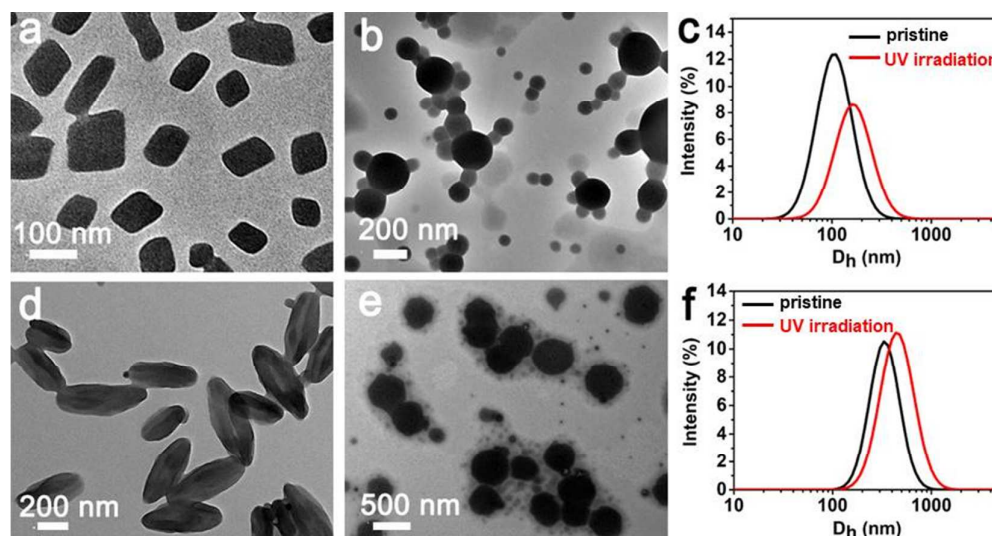


**Figure S14.** TEM images of the $PMAA_{112}$-*b*-$PMAAz_n$ nanoparticles at different conditions: a) and d) pristine, b) and e) after UV irradiation. c) and f) The respective corresponding particle size and distribution obtained from the DLS measurements. For a-c), $PMAA_{112}$-*b*-$PMAAz_{66}$, and for d~f), $PMAA_{112}$-*b*-$PMAAz_{142}$, respectively.

# 4. References

[1] Y. Tian, K. Watanabe, X. Kong, J. Abe, T. Iyoda, *Macromolecules* **2002**, *35*, 3739-3747.

[2] Q. Li, Y. Bao, H. Wang, F. Du, Q. Li, B. Jin, R. Bai, *Polym. Chem.* **2013**, *4*, 2891-2897.